Sciencexpress Research Articles

Toddler: An Embryonic Signal That Promotes Cell Movement via Apelin Receptors

Andrea Pauli,[1]* Megan L. Norris,[1]† Eivind Valen,[1]† Guo-Liang Chew,[1] James A. Gagnon,[1] Steven Zimmerman,[1] Andrew Mitchell,[2] Jiao Ma,[2] Julien Dubrulle,[1] Deepak Reyon,[3,4] Shengdar Q. Tsai,[3,4] J. Keith Joung,[3,4,5] Alan Saghatelian,[2] Alexander F. Schier[1,5,6,7]*

[1]Department of Molecular and Cellular Biology, Harvard University, MA 02138, USA. [2]Department of Chemistry and Chemical Biology, Harvard University, MA 02138, USA. [3]Molecular Pathology Unit, Center for Computational and Integrative Biology, and Center for Cancer Research, Massachusetts General Hospital, Charlestown, MA 02129, USA. [4]Department of Pathology, Harvard Medical School, Boston, MA 02115, USA. [5]The Broad Institute of Massachusetts Institute of Technology and Harvard, Cambridge, MA 02142, USA. [6]FAS Center for Systems Biology, Harvard University, Cambridge, MA 02138, USA. [7]Center for Brain Science, Harvard University, Cambridge, MA 02138, USA.

*Corresponding author. E-mail: pauli@fas.harvard.edu (A.P.); schier@fas.harvard.edu (A.F.S.)

†These authors contributed equally to this work.

It has been assumed that most if not all signals regulating early development have been identified. Contrary to this expectation, we identified 28 candidate signaling proteins expressed during zebrafish embryogenesis, including Toddler, a short, conserved, and secreted peptide. Both absence and over-production of Toddler reduce the movement of mesendodermal cells during zebrafish gastrulation. Local and ubiquitous production of Toddler promote cell movement, suggesting that Toddler is neither an attractant nor a repellent but acts globally as a motogen. Toddler drives internalization of G-protein-coupled APJ/Apelin receptors, and activation of APJ/Apelin signaling rescues *toddler* mutants. These results indicate that Toddler is an activator of APJ/Apelin receptor signaling, promotes gastrulation movements, and might be the first in a series of uncharacterized developmental signals.

Many of the inductive events during early development are directed by a small number of signaling pathways whose agonists have been known for more than a decade (*1*). Therefore, it has been assumed that most if not all embryonic signals have been identified. However, the molecular control of some embryonic processes is still poorly understood. For example, it is largely unclear how cell migration is regulated during gastrulation or how cells coalesce into discrete tissues during organogenesis (*2*–*5*), suggesting that some of the involved signals are yet to be identified. Moreover, recent genomic studies have suggested that translation of short open reading frames and the generation of small peptides is much more pervasive than previously assumed (*6*, *7*). To search for new candidate signaling molecules, we used the Translated ORF Classifier (TOC) (*7*) to examine zebrafish RNA-Seq and ribosome profiling datasets (*7*–*9*) for non-annotated translated open reading frames (ORFs) (Fig. 1A and supplementary materials, materials and methods). This analysis identified 700 novel protein-coding transcripts (399 loci) (data files S1 and S2), of which 81% (562 transcripts in 325 loci) shared nucleotide sequence alignments with other vertebrates (table S1). Notably, this approach identified 28 candidate signaling proteins (40 transcript isoforms) characterized by the presence of putative signal sequences and lack of predicted trans-membrane domains (table S1). Ribosome profiling and phylogenetic analysis suggest that these RNAs can generate secreted peptides with lengths ranging from 32 to 556 amino acids (Fig. 1A, fig. S1, and table S1). Although these genes have not been identified previously or are annotated in the zebrafish Ensembl database as non-coding RNAs, the majority (24/28) appear to be conserved in other vertebrates (fig. S1 and table S1).

Toddler Encodes a Short, Conserved, and Secreted Peptide

To test the functional potential of these candidate signals, we focused on a gene that we named *toddler* based on the phenotype described below (Fig. 1B). *Toddler* (*tdl*) mRNA is expressed ubiquitously during late blastula and gastrula stages and becomes restricted to the lateral mesoderm, endoderm, and anterior and posterior notochord after gastrulation (Fig. 1C). *Toddler* is annotated as a non-coding RNA in zebrafish (*ENSDARG00000094729*), mouse (*Gm10664;* also called *EndE* (*10*)) and human (*LOC100506013*) (fig. S2), and is present in two lncRNA catalogs (*9*, *11*); however, it contains a 58 amino acid open reading frame with a predicted signal sequence and high conservation in vertebrates, including human (Fig. 1D; fig. S3). Sequence comparisons with the highly conserved C-terminal portion did not identify homology to any other known proteins, raising the possibility that this gene encodes an uncharacterized embryonic signal.

Six lines of evidence indicate that *toddler* is translated and encodes a secreted peptide. First, phylogenetic comparisons of synonymous versus non-synonymous codon changes reveal strong amino acid preservation in the *toddler* ORF (PhyloCSF score of 98; see Fig. 1, B and D, and table S1). Second, previous ribosome profiling data in mouse (*6*) and zebrafish (*7*) indicate that the *toddler* ORF is protected by actively translating ribosomes in vivo (Fig. 1B). Third, mass-spectrometric analysis of non-trypsinated protein extracts from embryos expressing *toddler* mRNA detected the 11 amino acid C-terminal Toddler peptide fragment that is predicted to be a convertase cleavage product (Fig. 1D and fig. S4). Fourth, eGFP fusion proteins containing the wild-type signal sequence of Toddler are found extracellularly, whereas signal peptide cleavage site mutants are retained in the cell (Fig. 1E). Fifth, as described below, extracellular injection of in vitro synthesized Toddler peptide (C-terminal 21 amino acids) elicits the same gain-of-function phenotypes as excess of *toddler* mRNA. Sixth, wild-type but not frame-shifted *toddler* mRNA rescues *toddler* mutants (see below), providing direct evidence that it is the peptide product rather than the RNA that is functional in vivo. Together, these findings identify Toddler as a short, conserved, and secreted peptide.

Toddler Is Essential for Embryogenesis

To disrupt *toddler* function, we generated mutants by TALEN-mediated mutagenesis (fig. S5 and Materials and Methods) (*12*, *13*). Seven *toddler* alleles were recovered, each of which introduces a frame shift immediately after the signal peptide sequence (fig. S5B,C). The vast majority of homozygous *toddler* mutants die between 5-7 days of development and display small or absent hearts, posterior accumulation of blood cells, malformed pharyngeal endoderm, and abnormal left-right positioning and formation of the liver (Fig. 2, A and B, and fig. S6). Penetrance and

expressivity of *toddler* mutants vary, including occasional escapers that live to adulthood and rare instances of *toddler* mutants that display more severe defects in endoderm and mesoderm formation (fig. S7). Notably, the lethality of *toddler* mutants (survival 0/25 animals) was rescued by injection of low amounts (2 pg) of wild-type (survival 23/30 animals) but not frame-shifted (survival 0/32 animals) *toddler* mRNA (Fig. 2, A, C, and D). Embryonically rescued *toddler* mutants survived to adulthood and were fertile in the absence of any later source of Toddler peptide, indicating that zebrafish Toddler is only essential during early embryogenesis.

Toddler is Required for Normal Gastrulation Movements

To determine when Toddler function is required during early embryogenesis, we used a heat-shock inducible transgene. Induction of *toddler* expression during late blastula and early gastrula stages, but not at later times, rescued *toddler* mutants (fig. S8 and Materials and Methods).

The early requirement for Toddler, together with its expression peak during gastrulation (Fig. 1C), suggested that the later phenotypes originate from earlier defects. We therefore analyzed morphology and gene expression during blastula and gastrula stages and discovered that *toddler* mutant mesendodermal progenitors did not move properly toward the animal pole during gastrulation. Although ventral and lateral mesendodermal cells in wild-type embryos internalized at the margin and moved toward the animal pole (Fig. 2, C and E), these cells were closely packed and confined to a band near the margin in *toddler* mutant embryos (Fig. 2, C and D, and fig. S9). These defects were apparent by analysis of endodermal (*sox17)* and mesodermal (*fibronectin1/fn1, spadetail/tbx16, fascin, draculin/drl)* markers (Fig. 2C and fig. S9). In contrast, ectodermal (*sox3*), dorsal mesodermal (*goosecoid/gsc, hgg1*) and tail mesodermal (*ntla*) markers were largely unchanged in their expression domains (fig. S10). In addition to the ventrolateral movement defects, *toddler* mutants contained ~ 20% fewer endodermal cells at mid-gastrulation (Fig. 2, C and D, and fig. S9A). The initial expression of mesendodermal markers appeared unaffected (fig. S10B), suggesting that mesendodermal cells are specified normally in *toddler* mutant embryos but proliferate less. Notably, the *toddler* gastrulation phenotypes could be rescued by injecting low levels (2 pg) of *toddler* mRNA at the one-cell stage (Fig. 2, C and D, and fig. S9, A and C). These results reveal an important role for Toddler in the movement of ventral and lateral mesendodermal cells during gastrulation.

Toddler Promotes Endodermal and Mesodermal Cell Migration

To determine how Toddler affects the movement of cells during gastrulation, we performed live cell imaging and followed cell trajectories in wild-type and *toddler* mutant embryos (movies S1 to S6). *Toddler* mutant endodermal cells (*sox17::GFP* (*14*)) displayed reduced movement toward the animal pole (Fig. 3A, fig. S11, and movies S1 and S2), migrated more slowly and showed reduced net (start-to-end) displacement compared to wild-type cells (Fig. 3B and fig. S11). During early gastrulation *toddler* mutant endodermal cells exhibited the characteristic random-walk-like migration pattern observed in wild-type embryos (*3*, *15*), but they migrated in a less directional fashion than their wild-type counterparts during later gastrulation (movie S1and Fig. 3B).

To analyze the earliest steps of mesendoderm movement, we followed the paths of H2B-RFP-labeled nuclei by light-sheet microscopy in wild-type and *toddler* mutant embryos (movie S3; fig. S12). Analysis of 10 wild-type and 11 *toddler* mutant embryos confirmed that the movement of ventrolateral but not dorsal internalizing cells toward the animal pole was impaired in *toddler* mutants (Fig. 3, C to I; figs. S12 to S14; and movies S3 to S6). Internalization of ventrolateral cells at the margin was delayed (Fig. 3C,D; fig. S13A; movies S4 and S5) and reduced (Fig. 3, E to G and I; fig. S13; and movies S3 to S6). Although internalization in wild-type embryos started about 30 min before embryos reached 50% epiboly, it often commenced only after the 50% epiboly stage in *toddler* mutants (Fig. 3, C and D; fig. S13A; and movies S4 and S5). Ventrolateral internalized cells moved more slowly (Fig. 3H,I) and often piled up at the margin (Fig. 3, C and E; figs. S13 to S15; and movies S3 to S6). In addition, epiboly movements were often delayed in *toddler* mutants, particularly during the time of internalization (fig. S13, A and B). In rare cases we observed an almost complete absence of animal pole-directed ventrolateral cell movements; in these embryos, ventral and lateral marginal cells instead moved vegetally (movies S3, S5, and S6), likely contributing to the ectopic accumulation of posteriorly located blood cells at later stages (Fig. 2, A and B). These results identify Toddler as a key signal that promotes the internalization and animal pole-directed movement of mesendodermal cells during gastrulation.

Overexpression of Toddler Phenocopies *toddler* Mutants

In contrast to inducers of specific cell fates, many signals involved in cell migration or tissue morphogenesis share loss- and gain-of-function phenotypes. For example, both reduction and increase in Wnt/planar cell polarity signaling disrupt convergence and extension movements during gastrulation (*2–5*). To determine whether Toddler might share this feature, we carried out overexpression analyses. Injection of *toddler* mRNA at levels only 5-times higher (≥ 10 pg) than needed for rescue caused phenotypes in wild-type embryos that resembled *toddler* loss-of-function mutants, including gastrulation and heart defects (Fig. 2, A,C, and D; fig. S9, A and C). Similar phenotypes were observed upon extracellular injection of an in vitro synthesized Toddler peptide fragment (C-terminal 21 amino acids) (fig. S16). These observations reveal that proper levels of Toddler are required for normal mesendodermal movement and provide further evidence of an important role for Toddler in cell migration.

Toddler Functions as a Motogen

Most genes encoding signals that attract or repel cells are expressed in specific domains (*16*), and ubiquitous production of such signals interferes with guided cell migration. In contrast, we find that *toddler* RNA is expressed ubiquitously (Fig. 1C and fig. S17A) and that ubiquitous expression of *toddler* mRNA upon injection at the one-cell stage promotes the normal movement of mesendodermal cells in *toddler* mutants (Fig. 2, C and D). To further test the role of Toddler in cell migration, we locally expressed Toddler in the vegetal or animal regions of *toddler* mutants. In both scenarios, localized Toddler production was able to promote the migration of mesendodermal cells and rescue *toddler* mutants (Fig. 4). Although more complex scenarios are formally possible [e.g., local processing (*17*), self-generated gradient formation (*18*, *19*)], these results suggest that Toddler does not attract cells to or repel cells from specific sites. Instead, Toddler appears to act as a motogen (*20–22*) - a general promoter of mesendodermal cell migration.

Toddler Acts via APJ/Apelin Receptors

To identify candidate receptors for Toddler, we compared the *toddler* phenotype to previously described receptor mutant phenotypes. Based on the small size of Toddler peptide and the involvement of G-protein signaling in gastrulation movements, we focused on GPCRs as candidate Toddler receptors (*14*, *23–30*). Four observations raised the possibility that the G-protein coupled Apelin/APJ receptor might mediate Toddler signaling. First, loss of Apelin/APJ receptor signaling results in small hearts and affects lateral mesoderm migration in zebrafish (*24–26*), phenotypes reminiscent of some aspects of the *toddler* mutant phenotype. However, in contrast to the broad roles of Toddler in mesendoderm migration, Apelin receptor signaling had been specifically implicated in cardiovascular development (*24–26*, *31–36*). Second, overexpression of Apelin, the only known ligand for the Apelin/APJ receptor (*35–38*), interferes with gastrulation movements in zebrafish (*24–26*). Third, the expression levels of Apelin receptors and Toddler peak during gastrula-

tion (Fig. 5A), and Apelin receptors are expressed in mesendodermal cells (fig. S16A) (*24*, *25*, *39*), the cell types affected in *toddler* mutants. Fourth, we found that Apelin is expressed only at the end of gastrulation (Fig. 5A) (*24*), after the *toddler* and *apelin/APJ receptor* phenotypes (*24*, *25*, *40*) are apparent. These observations, together with the milder phenotypes observed in the absence of Apelin as compared to loss of Apelin/APJ receptors (*24–26*, *34*, *36*, *41–46*) raised the hypothesis that Toddler might be the bona fide activator of Apelin/APJ receptor signaling during gastrulation. We tested three predictions of this model.

First, we determined whether the absence of Apelin receptor function phenocopies *toddler* mutants. We re-examined *aplnra* and *aplnrb* double morphants (*24–26*) and found phenotypes that were highly similar to *toddler* mutants, including reduced movement of ventrolateral mesendoderm during gastrulation (Fig. 5, B and C). We also confirmed and extended previous analyses of the effects of Apelin overexpression (*24–26*) and found defects very similar to those caused by Toddler overexpression (Fig. 5, B and C). In addition, we observed that co-expression of Toddler and Apelin receptor at levels that individually did not cause major defects resulted in abnormal gastrulation movements reminiscent of Toddler and Apelin (*24–26*) overexpression phenotypes (Fig. 5D). These results reveal shared morphogenetic activities of the Apelin receptor and Toddler signaling pathways.

Second, we tested the epistatic relationship between Toddler and Apelin receptor signaling. The similarity of gain- and loss-of-function phenotypes precluded standard tests such as overexpression of Toddler in Apelin receptor mutants. Instead, we tested whether activation of Apelin receptor signaling can bypass the requirement for Toddler. *Apelin* mRNA injection into *toddler* mutant embryos restored normal mesendoderm migration (Fig. 5, B and C), cardiac development and survival to adulthood. These results suggest that Toddler and Apelin activate the same signaling pathway.

Third, we tested whether Toddler can drive the internalization of Apelin receptors (Fig. 6), a hallmark of activated GPCR signaling (*47–50*). We misexpressed *toddler* mRNA with eGFP-tagged Apelin receptor a or b and observed strong internalization of the receptors from the plasma membrane (Fig. 6B). This effect was specific because other signaling proteins (chemokines Sdf1a/Cxcl12a or Sdf1b/Cxcl12b) did not alter the distribution of membrane-bound Apelin receptors, nor did Toddler alter the distribution of other chemokine receptors (Cxcr4a-eGFP, Cxcr4b-eGFP, Cxcr7b-eGFP) (Fig. 6B and fig. S18). Moreover, Toddler produced from a local clone of cells was sufficient to cause Aplnrb-eGFP internalization at a distance from the source, suggesting that secreted Toddler peptide can act on neighboring cells (Fig. 6C). This conclusion was further strengthened by the observation that extracellular injection of in vitro synthesized C-terminal Toddler or Apelin peptides induced efficient internalization of Aplnr-eGFP (Fig. 6D). These results indicate that Toddler activates Apelin receptors.

Discussion

Our study indicates that Toddler is an activator of APJ/Apelin receptor signaling, promotes gastrulation movements (see summary in Fig. 6E), and may be the first in a series of previously unknown developmental signals. While this study was under review, Toddler (named ELABELA) was independently reported to signal via APJ/Apelin receptors during endoderm differentiation and heart formation (*51*). Our results lead to four major conclusions.

First, Toddler is a previously unrecognized signal that promotes cell movement during gastrulation. The rescue of *toddler* mutants by ubiquitous Toddler expression suggests that Toddler acts neither as a chemoattractant nor –repellant, but rather as a non-directional signal to promote the internalization and movement of ventrolateral mesendodermal cells. Dorsal mesendoderm movement is largely unaffected in *toddler* mutants, consistent with the absence of Apelin receptor expression in this region, and the role of other pathways in dorsal gastrulation movements (*3*). Both loss and over-production of Toddler reduce cell movement, revealing that Toddler levels need to be tightly regulated to allow for normal gastrulation. It remains to be determined whether Toddler promotes motility by regulating cell shape, cellular protrusions, cell-substrate interactions, cell-cell adhesion or through other means.

Second, Toddler-Apelin receptor signaling provides a long-sought link between mesendoderm induction and migration. Nodal signaling not only induces mesendoderm formation (*52*) but also activates the expression of Apelin receptors (fig. S17B) (*39*).Thus, Nodal-mediated induction of Apelin receptor expression might render cells competent to respond to Toddler and to become more motile (Fig. 6E). In this scenario, the activation of Apelin receptor expression in cells located at the margin at the end of the blastula stage would restrict the motogenic effects of Toddler and prevent ectopic and premature cell motility.

Third, Toddler is a novel agonist of Apelin receptor signaling, as evidenced by Toddler-induced internalization of APJ/Apelin receptors and rescue of *toddler* mutants by production of the known receptor agonist Apelin. Additionally, a fusion protein of alkaline phosphatase and Toddler binds to cells expressing Apelin receptors (*51*). Previous studies have implicated Apelin receptor signaling in a variety of biological processes, including the regulation of cardiovascular development and physiology, the control of fluid homeostasis, or even as a co-receptor for HIV infection (*53*, *54*). Although Apelin has previously been the only known agonist of the Apelin/APJ receptor, genetic studies have found discrepancies between the roles of Apelin and its receptor in mouse (*34*, *36*, *45*, *55*, *56*) and zebrafish (*24–26*). For example, Apelin knockout mice are viable and fertile (*45*, *46*, *57*) whereas Apelin/APJ receptor mutant mice are born at sub-Mendelian ratios (*34*). Our studies suggest that both Toddler and Apelin can activate Apelin/APJ receptors and indicate that it is endogenous Toddler - not Apelin - that activates Apelin receptor signaling during zebrafish gastrulation. Analogously to the promise of Apelin in biomedical applications (*53*, *54*), Toddler and its derivatives may take the place of Apelin in therapeutic contexts. Indeed, Toddler may also activate mammalian Apelin receptors since misexpression of zebrafish, mouse and human Toddler induces similar overexpression phenotypes in zebrafish (fig. S19).

Fourth, our RNA-Seq and ribosome profiling data indicate that Toddler might just be one of several poorly characterized developmental signals that may have been missed in mutagenesis screens due to their small size. Applying similar genomic approaches to adult tissues might identify additional previously unknown signals that regulate physiological and behavioral processes.

References and Notes

1. B. Alberts *et al*., *Molecular Biology of the Cell* (Garland Science, ed. 5, 2007).
2. C.-P. Heisenberg, Y. Bellaïche, Forces in tissue morphogenesis and patterning. *Cell* **153**, 948–962 (2013). doi:10.1016/j.cell.2013.05.008 Medline
3. L. Solnica-Krezel, D. S. Sepich, Gastrulation: making and shaping germ layers. *Annu. Rev. Cell Dev. Biol.* **28**, 687–717 (2012). doi:10.1146/annurev-cellbio-092910-154043 Medline
4. J. B. Wallingford, Planar cell polarity and the developmental control of cell behavior in vertebrate embryos. *Annu. Rev. Cell Dev. Biol.* **28**, 627–653 (2012). doi:10.1146/annurev-cellbio-092910-154208 Medline
5. S. Nowotschin, A.-K. Hadjantonakis, Cellular dynamics in the early mouse embryo: from axis formation to gastrulation. *Curr. Opin. Genet. Dev.* **20**, 420–427 (2010). doi:10.1016/j.gde.2010.05.008 Medline
6. N. T. Ingolia, L. F. Lareau, J. S. Weissman, Ribosome profiling of mouse embryonic stem cells reveals the complexity and dynamics of mammalian proteomes. *Cell* **147**, 789–802 (2011). doi:10.1016/j.cell.2011.10.002 Medline
7. G.-L. Chew, A. Pauli, J. L. Rinn, A. Regev, A. F. Schier, E. Valen, Ribosome profiling reveals resemblance between long non-coding RNAs and 5′ leaders of coding RNAs. *Development* **140**, 2828–2834 (2013). doi:10.1242/dev.098343 Medline
8. A. Pauli, E. Valen, M. F. Lin, M. Garber, N. L. Vastenhouw, J. Z. Levin, L.

Fan, A. Sandelin, J. L. Rinn, A. Regev, A. F. Schier, Systematic identification of long noncoding RNAs expressed during zebrafish embryogenesis. *Genome Res.* **22**, 577–591 (2012). doi:10.1101/gr.133009.111 Medline
9. I. Ulitsky, A. Shkumatava, C. H. Jan, H. Sive, D. P. Bartel, Conserved function of lincRNAs in vertebrate embryonic development despite rapid sequence evolution. *Cell* **147**, 1537–1550 (2011). doi:10.1016/j.cell.2011.11.055 Medline
10. A. S. Hassan, J. Hou, W. Wei, P. A. Hoodless, Expression of two novel transcripts in the mouse definitive endoderm. *Gene Expr. Patterns* **10**, 127–134 (2010). doi:10.1016/j.gep.2010.02.001 Medline
11. M. Guttman, J. Donaghey, B. W. Carey, M. Garber, J. K. Grenier, G. Munson, G. Young, A. B. Lucas, R. Ach, L. Bruhn, X. Yang, I. Amit, A. Meissner, A. Regev, J. L. Rinn, D. E. Root, E. S. Lander, lincRNAs act in the circuitry controlling pluripotency and differentiation. *Nature* **477**, 295–300 (2011). doi:10.1038/nature10398 Medline
12. D. Reyon, S. Q. Tsai, C. Khayter, J. A. Foden, J. D. Sander, J. K. Joung, FLASH assembly of TALENs for high-throughput genome editing. *Nat. Biotechnol.* **30**, 460–465 (2012). doi:10.1038/nbt.2170 Medline
13. J. D. Sander, L. Cade, C. Khayter, D. Reyon, R. T. Peterson, J. K. Joung, J. R. Yeh, Targeted gene disruption in somatic zebrafish cells using engineered TALENs. *Nat. Biotechnol.* **29**, 697–698 (2011). doi:10.1038/nbt.1934 Medline
14. T. Mizoguchi, H. Verkade, J. K. Heath, A. Kuroiwa, Y. Kikuchi, Sdf1/Cxcr4 signaling controls the dorsal migration of endodermal cells during zebrafish gastrulation. *Development* **135**, 2521–2529 (2008). doi:10.1242/dev.020107 Medline
15. G. Pézeron, P. Mourrain, S. Courty, J. Ghislain, T. S. Becker, F. M. Rosa, N. B. David, Live analysis of endodermal layer formation identifies random walk as a novel gastrulation movement. *Curr. Biol.* **18**, 276–281 (2008). doi:10.1016/j.cub.2008.01.028 Medline
16. M. Doitsidou, M. Reichman-Fried, J. Stebler, M. Köprunner, J. Dörries, D. Meyer, C. V. Esguerra, T. Leung, E. Raz, Guidance of primordial germ cell migration by the chemokine SDF-1. *Cell* **111**, 647–659 (2002). doi:10.1016/S0092-8674(02)01135-2 Medline
17. M. Haskel-Ittah, D. Ben-Zvi, M. Branski-Arieli, E. D. Schejter, B. Z. Shilo, N. Barkai, Self-organized shuttling: generating sharp dorsoventral polarity in the early Drosophila embryo. *Cell* **150**, 1016–1028 (2012). doi:10.1016/j.cell.2012.06.044 Medline
18. G. Venkiteswaran, S. W. Lewellis, J. Wang, E. Reynolds, C. Nicholson, H. Knaut, Generation and dynamics of an endogenous, self-generated signaling gradient across a migrating tissue. *Cell* **155**, 674–687 (2013). doi:10.1016/j.cell.2013.09.046 Medline
19. E. Donà, J. D. Barry, G. Valentin, C. Quirin, A. Khmelinskii, A. Kunze, S. Durdu, L. R. Newton, A. Fernandez-Minan, W. Huber, M. Knop, D. Gilmour, Directional tissue migration through a self-generated chemokine gradient. *Nature* **503**, 285–289 (2013). Medline
20. E. M. Powell, W. M. Mars, P. Levitt, Hepatocyte growth factor/scatter factor is a motogen for interneurons migrating from the ventral to dorsal telencephalon. *Neuron* **30**, 79–89 (2001). doi:10.1016/S0896-6273(01)00264-1 Medline
21. P. Giacobini, A. Messina, S. Wray, C. Giampietro, T. Crepaldi, P. Carmeliet, A. Fasolo, Hepatocyte growth factor acts as a motogen and guidance signal for gonadotropin hormone-releasing hormone-1 neuronal migration. *J. Neurosci.* **27**, 431–445 (2007). doi:10.1523/JNEUROSCI.4979-06.2007 Medline
22. G. Kirfel, B. Borm, A. Rigort, V. Herzog, The secretory beta-amyloid precursor protein is a motogen for human epidermal keratinocytes. *Eur. J. Cell Biol.* **81**, 664–676 (2002). doi:10.1078/0171-9335-00284 Medline
23. S. Nair, T. F. Schilling, Chemokine signaling controls endodermal migration during zebrafish gastrulation. *Science* **322**, 89–92 (2008). doi:10.1126/science.1160038 Medline
24. X.-X. I. Zeng, T. P. Wilm, D. S. Sepich, L. Solnica-Krezel, Apelin and its receptor control heart field formation during zebrafish gastrulation. *Dev. Cell* **12**, 391–402 (2007). doi:10.1016/j.devcel.2007.01.011 Medline
25. I. C. Scott, B. Masri, L. A. D'Amico, S. W. Jin, B. Jungblut, A. M. Wehman, H. Baier, Y. Audigier, D. Y. Stainier, The g protein-coupled receptor agtrl1b regulates early development of myocardial progenitors. *Dev. Cell* **12**, 403–413 (2007). doi:10.1016/j.devcel.2007.01.012 Medline
26. S. Paskaradevan, I. C. Scott, The Aplnr GPCR regulates myocardial progenitor development via a novel cell-non-autonomous, Gα(i/o) protein-independent pathway. *Biol. Open* **1**, 275–285 (2012). doi:10.1242/bio.2012380 Medline
27. X. Li, I. Roszko, D. S. Sepich, M. Ni, H. E. Hamm, F. L. Marlow, L. Solnica-Krezel, Gpr125 modulates Dishevelled distribution and planar cell polarity signaling. *Development* **140**, 3028–3039 (2013). doi:10.1242/dev.094839 Medline
28. F. Lin, S. Chen, D. S. Sepich, J. R. Panizzi, S. G. Clendenon, J. A. Marrs, H. E. Hamm, L. Solnica-Krezel, Galpha12/13 regulate epiboly by inhibiting E-cadherin activity and modulating the actin cytoskeleton. *J. Cell Biol.* **184**, 909–921 (2009). doi:10.1083/jcb.200805148 Medline
29. M. Costa, E. T. Wilson, E. Wieschaus, A putative cell signal encoded by the folded gastrulation gene coordinates cell shape changes during Drosophila gastrulation. *Cell* **76**, 1075–1089 (1994). doi:10.1016/0092-8674(94)90384-0 Medline
30. S. Parks, E. Wieschaus, The Drosophila gastrulation gene concertina encodes a G alpha-like protein. *Cell* **64**, 447–458 (1991). doi:10.1016/0092-8674(91)90652-F Medline
31. C. D'Aniello, E. Lonardo, S. Iaconis, O. Guardiola, A. M. Liguoro, G. L. Liguori, M. Autiero, P. Carmeliet, G. Minchiotti, G protein-coupled receptor APJ and its ligand apelin act downstream of Cripto to specify embryonic stem cells toward the cardiac lineage through extracellular signal-regulated kinase/p70S6 kinase signaling pathway. *Circ. Res.* **105**, 231–238 (2009). doi:10.1161/CIRCRESAHA.109.201186 Medline
32. I.-N. E. Wang, X. Wang, X. Ge, J. Anderson, M. Ho, E. Ashley, J. Liu, M. J. Butte, M. Yazawa, R. E. Dolmetsch, T. Quertermous, P. C. Yang, Apelin enhances directed cardiac differentiation of mouse and human embryonic stem cells. *PLoS ONE* **7**, e38328 (2012). doi:10.1371/journal.pone.0038328 Medline
33. D. Tempel, M. de Boer, E. D. van Deel, R. A. Haasdijk, D. J. Duncker, C. Cheng, S. Schulte-Merker, H. J. Duckers, Apelin enhances cardiac neovascularization after myocardial infarction by recruiting aplnr+ circulating cells. *Circ. Res.* **111**, 585–598 (2012). doi:10.1161/CIRCRESAHA.111.262097 Medline
34. Y. Kang, J. Kim, J. P. Anderson, J. Wu, S. R. Gleim, R. K. Kundu, D. L. McLean, J. D. Kim, H. Park, S. W. Jin, J. Hwa, T. Quertermous, H. J. Chun, Apelin-APJ signaling is a critical regulator of endothelial MEF2 activation in cardiovascular development. *Circ. Res.* **113**, 22–31 (2013). doi:10.1161/CIRCRESAHA.113.301324 Medline
35. M. Inui, A. Fukui, Y. Ito, M. Asashima, Xapelin and Xmsr are required for cardiovascular development in Xenopus laevis. *Dev. Biol.* **298**, 188–200 (2006). doi:10.1016/j.ydbio.2006.06.028 Medline
36. D. N. Charo, M. Ho, G. Fajardo, M. Kawana, R. K. Kundu, A. Y. Sheikh, T. P. Finsterbach, N. J. Leeper, K. V. Ernst, M. M. Chen, Y. D. Ho, H. J. Chun, D. Bernstein, E. A. Ashley, T. Quertermous, Endogenous regulation of cardiovascular function by apelin-APJ. *Am. J. Physiol. Heart Circ. Physiol.* **297**, H1904–H1913 (2009). doi:10.1152/ajpheart.00686.2009 Medline
37. K. Tatemoto, M. Hosoya, Y. Habata, R. Fujii, T. Kakegawa, M. X. Zou, Y. Kawamata, S. Fukusumi, S. Hinuma, C. Kitada, T. Kurokawa, H. Onda, M. Fujino, Isolation and characterization of a novel endogenous peptide ligand for the human APJ receptor. *Biochem. Biophys. Res. Commun.* **251**, 471–476 (1998). doi:10.1006/bbrc.1998.9489 Medline
38. D. K. Lee, R. Cheng, T. Nguyen, T. Fan, A. P. Kariyawasam, Y. Liu, D. H. Osmond, S. R. George, B. F. O'Dowd, Characterization of apelin, the ligand for the APJ receptor. *J. Neurochem.* **74**, 34–41 (2000). doi:10.1046/j.1471-4159.2000.0740034.x Medline
39. B. Tucker, C. Hepperle, D. Kortschak, B. Rainbird, S. Wells, A. C. Oates, M. Lardelli, Zebrafish Angiotensin II Receptor-like 1a (agtrl1a) is expressed in migrating hypoblast, vasculature, and in multiple embryonic epithelia. *Gene Expr. Patterns* **7**, 258–265 (2007). doi:10.1016/j.modgep.2006.09.006 Medline
40. S. Nornes, B. Tucker, M. Lardelli, Zebrafish aplnra functions in epiboly. *BMC Res. Notes* **2**, 231 (2009). doi:10.1186/1756-0500-2-231 Medline
41. M. C. Scimia, C. Hurtado, S. Ray, S. Metzler, K. Wei, J. Wang, C. E. Woods, N. H. Purcell, D. Catalucci, T. Akasaka, O. F. Bueno, G. P. Vlasuk, P. Kaliman, R. Bodmer, L. H. Smith, E. Ashley, M. Mercola, J. H. Brown, P. Ruiz-Lozano, APJ acts as a dual receptor in cardiac hypertrophy. *Nature* **488**, 394–398 (2012). doi:10.1038/nature11263 Medline
42. J. Ishida, T. Hashimoto, Y. Hashimoto, S. Nishiwaki, T. Iguchi, S. Harada, T.

Sugaya, H. Matsuzaki, R. Yamamoto, N. Shiota, H. Okunishi, M. Kihara, S. Umemura, F. Sugiyama, K. Yagami, Y. Kasuya, N. Mochizuki, A. Fukamizu, Regulatory roles for APJ, a seven-transmembrane receptor related to angiotensin-type 1 receptor in blood pressure in vivo. *J. Biol. Chem.* **279**, 26274–26279 (2004). doi:10.1074/jbc.M404149200 Medline
43. E. M. Roberts, M. J. Newson, G. R. Pope, R. Landgraf, S. J. Lolait, A. M. O'Carroll, Abnormal fluid homeostasis in apelin receptor knockout mice. *J. Endocrinol.* **202**, 453–462 (2009). doi:10.1677/JOE-09-0134 Medline
44. H. Kidoya, M. Ueno, Y. Yamada, N. Mochizuki, M. Nakata, T. Yano, R. Fujii, N. Takakura, Spatial and temporal role of the apelin/APJ system in the caliber size regulation of blood vessels during angiogenesis. *EMBO J.* **27**, 522–534 (2008). doi:10.1038/sj.emboj.7601982 Medline
45. K. Kuba, L. Zhang, Y. Imai, S. Arab, M. Chen, Y. Maekawa, M. Leschnik, A. Leibbrandt, M. Markovic, J. Schwaighofer, N. Beetz, R. Musialek, G. G. Neely, V. Komnenovic, U. Kolm, B. Metzler, R. Ricci, H. Hara, A. Meixner, M. Nghiem, X. Chen, F. Dawood, K. M. Wong, R. Sarao, E. Cukerman, A. Kimura, L. Hein, J. Thalhammer, P. P. Liu, J. M. Penninger, Impaired heart contractility in Apelin gene-deficient mice associated with aging and pressure overload. *Circ. Res.* **101**, e32–e42 (2007). doi:10.1161/CIRCRESAHA.107.158659 Medline
46. A. Y. Sheikh, H. J. Chun, A. J. Glassford, R. K. Kundu, I. Kutschka, D. Ardigo, S. L. Hendry, R. A. Wagner, M. M. Chen, Z. A. Ali, P. Yue, D. T. Huynh, A. J. Connolly, M. P. Pelletier, P. S. Tsao, R. C. Robbins, T. Quertermous, In vivo genetic profiling and cellular localization of apelin reveals a hypoxia-sensitive, endothelial-centered pathway activated in ischemic heart failure. *Am. J. Physiol. Heart Circ. Physiol.* **294**, H88–H98 (2008). doi:10.1152/ajpheart.00935.2007 Medline
47. N. A. Evans, D. A. Groarke, J. Warrack, C. J. Greenwood, K. Dodgson, G. Milligan, S. Wilson, Visualizing differences in ligand-induced beta-arrestin-GFP interactions and trafficking between three recently characterized G protein-coupled receptors. *J. Neurochem.* **77**, 476–485 (2001). doi:10.1046/j.1471-4159.2001.00269.x Medline
48. D. K. Lee, S. S. G. Ferguson, S. R. George, B. F. O'Dowd, The fate of the internalized apelin receptor is determined by different isoforms of apelin mediating differential interaction with beta-arrestin. *Biochem. Biophys. Res. Commun.* **395**, 185–189 (2010). doi:10.1016/j.bbrc.2010.03.151 Medline
49. A. Reaux, N. De Mota, I. Skultetyova, Z. Lenkei, S. El Messari, K. Gallatz, P. Corvol, M. Palkovits, C. Llorens-Cortès, Physiological role of a novel neuropeptide, apelin, and its receptor in the rat brain. *J. Neurochem.* **77**, 1085–1096 (2001). doi:10.1046/j.1471-4159.2001.00320.x Medline
50. N. Zhou, X. Fan, M. Mukhtar, J. Fang, C. A. Patel, G. C. DuBois, R. J. Pomerantz, Cell-cell fusion and internalization of the CNS-based, HIV-1 co-receptor, APJ. *Virology* **307**, 22–36 (2003). doi:10.1016/S0042-6822(02)00021-1 Medline
51. S. C. Chng, L. Ho, J. Tian, B. Reversade, ELABELA: A Hormone Essential for Heart Development Signals via the Apelin Receptor. *Dev. Cell* **27**, 672–680 (2013). doi:10.1016/j.devcel.2013.11.002 Medline
52. A. F. Schier, W. S. Talbot, Molecular genetics of axis formation in zebrafish. *Annu. Rev. Genet.* **39**, 561–613 (2005). doi:10.1146/annurev.genet.37.110801.143752 Medline
53. G. Barnes, A. G. Japp, D. E. Newby, Translational promise of the apelin—APJ system. *Heart* **96**, 1011–1016 (2010). doi:10.1136/hrt.2009.191122 Medline
54. M. J. Kleinz, A. P. Davenport, Emerging roles of apelin in biology and medicine. *Pharmacol. Ther.* **107**, 198–211 (2005). doi:10.1016/j.pharmthera.2005.04.001 Medline
55. A. Kasai, N. Shintani, H. Kato, S. Matsuda, F. Gomi, R. Haba, H. Hashimoto, M. Kakuda, Y. Tano, A. Baba, Retardation of retinal vascular development in apelin-deficient mice. *Arterioscler. Thromb. Vasc. Biol.* **28**, 1717–1722 (2008). doi:10.1161/ATVBAHA.108.163402 Medline
56. M. C. Scimia, C. Hurtado, S. Ray, S. Metzler, K. Wei, J. Wang, C. E. Woods, N. H. Purcell, D. Catalucci, T. Akasaka, O. F. Bueno, G. P. Vlasuk, P. Kaliman, R. Bodmer, L. H. Smith, E. Ashley, M. Mercola, J. H. Brown, P. Ruiz-Lozano, APJ acts as a dual receptor in cardiac hypertrophy. *Nature* **488**, 394–398 (2012). doi:10.1038/nature11263 Medline
57. H. Kidoya, H. Naito, N. Takakura, Apelin induces enlarged and nonleaky blood vessels for functional recovery from ischemia. *Blood* **115**, 3166–3174 (2010). doi:10.1182/blood-2009-07-232306 Medline
58. T. N. Petersen, S. Brunak, G. von Heijne, H. Nielsen, SignalP 4.0: discriminating signal peptides from transmembrane regions. *Nat. Methods* **8**, 785–786 (2011). doi:10.1038/nmeth.1701 Medline
59. L. Käll, A. Krogh, E. L. L. Sonnhammer, A combined transmembrane topology and signal peptide prediction method. *J. Mol. Biol.* **338**, 1027–1036 (2004). doi:10.1016/j.jmb.2004.03.016 Medline
60. L. Käll, A. Krogh, E. L. L. Sonnhammer, Advantages of combined transmembrane topology and signal peptide prediction—the Phobius web server. *Nucleic Acids Res.* **35**, (Web Server), W429–W432 (2007). doi:10.1093/nar/gkm256 Medline
61. M. F. Lin, I. Jungreis, M. Kellis, PhyloCSF: a comparative genomics method to distinguish protein coding and non-coding regions. *Bioinformatics* **27**, i275–i282 (2011). doi:10.1093/bioinformatics/btr209 Medline
62. C. B. Kimmel, W. W. Ballard, S. R. Kimmel, B. Ullmann, T. F. Schilling, Stages of embryonic development of the zebrafish. *Dev. Dyn.* **203**, 253–310 (1995). doi:10.1002/aja.1002030302 Medline
63. B. Boldajipour, H. Mahabaleshwar, E. Kardash, M. Reichman-Fried, H. Blaser, S. Minina, D. Wilson, Q. Xu, E. Raz, Control of chemokine-guided cell migration by ligand sequestration. *Cell* **132**, 463–473 (2008). doi:10.1016/j.cell.2007.12.034 Medline
64. M. D. Abramoff, P. J. Magalhães, S. J. Ram, Image processing with ImageJ. *Biophoton. Int.* **11**, 36–42 (2004).
65. C. Thisse, B. Thisse, High-resolution in situ hybridization to whole-mount zebrafish embryos. *Nat. Protoc.* **3**, 59–69 (2008). doi:10.1038/nprot.2007.514 Medline
66. A. Kaufmann, M. Mickoleit, M. Weber, J. Huisken, Multilayer mounting enables long-term imaging of zebrafish development in a light sheet microscope. *Development* **139**, 3242–3247 (2012). doi:10.1242/dev.082586 Medline
67. P. J. Keller, A. D. Schmidt, J. Wittbrodt, E. H. K. Stelzer, Digital scanned laser light-sheet fluorescence microscopy (DSLM) of zebrafish and Drosophila embryonic development. *Cold Spring Harb. Protoc.* **2011**, 1235–1243 (2011). doi:10.1101/pdb.prot065839 Medline
68. K. Jaqaman, D. Loerke, M. Mettlen, H. Kuwata, S. Grinstein, S. L. Schmid, G. Danuser, Robust single-particle tracking in live-cell time-lapse sequences. *Nat. Methods* **5**, 695–702 (2008). doi:10.1038/nmeth.1237 Medline

Acknowledgments: We thank D. Richardson and C. Kraft from the Harvard Center for Biological Imaging for technical support, F. Merkle for providing human and mouse ESC cDNA, M. Lin for the initial PhyloCSF analysis, L. Solnica-Krezel, E. Raz, C. Houart, members of the 2013 MBL Zebrafish Course, and the Schier lab for helpful discussions, and S. Mango, W. Talbot, R. Losick, J. Farrell, and K. Rogers for comments on the manuscript. Obtaining the TALEN plasmids will require the completion of a Uniform Biological Material Transfer Agreement (UBMTA) with the Massachusetts General Hospital. The Massachusetts General Hospital has applied for a patent that covers the FLASH method used to make the TALENs and JKJ is an inventor on this patent. JKJ has financial interests in Editas Medicine and Transposagen Biopharmaceuticals. JKJ is a member of the Scientific Advisory Board of Transposagen Biopharmaceuticals and is a co-founder and paid consultant of Editas Medicine and holds equity in both companies. JKJ's interests were reviewed and are managed by Massachusetts General Hospital and Partners HealthCare in accordance with their conflict of interest policies. This research was supported by NIH (AFS, AP, AS), HFSP (AP, EV), HHMI (G-LC) and the American Cancer Society (JAG). AP and AFS conceived the study and wrote the paper. AP collected and analyzed the data, with contributions from AFS, MLN (phenotypic characterization), EV (computational analyses), G-LC (ribosome profiling), JAG, SZ, DR, SQT, JKJ (TALEN-mediated mutagenesis), AM, JM, AS (mass spec), and JD (MATLAB cell tracking).

Supplementary Materials
www.sciencemag.org/content/science.1248636/DC1
Materials and Methods
Figs. S1 to S19
References (*58–68*)
Table S1
Data files S1 and S2

18 November 2013; accepted 26 December 2013
Published online 9 January 2014
10.1126/science.1248636

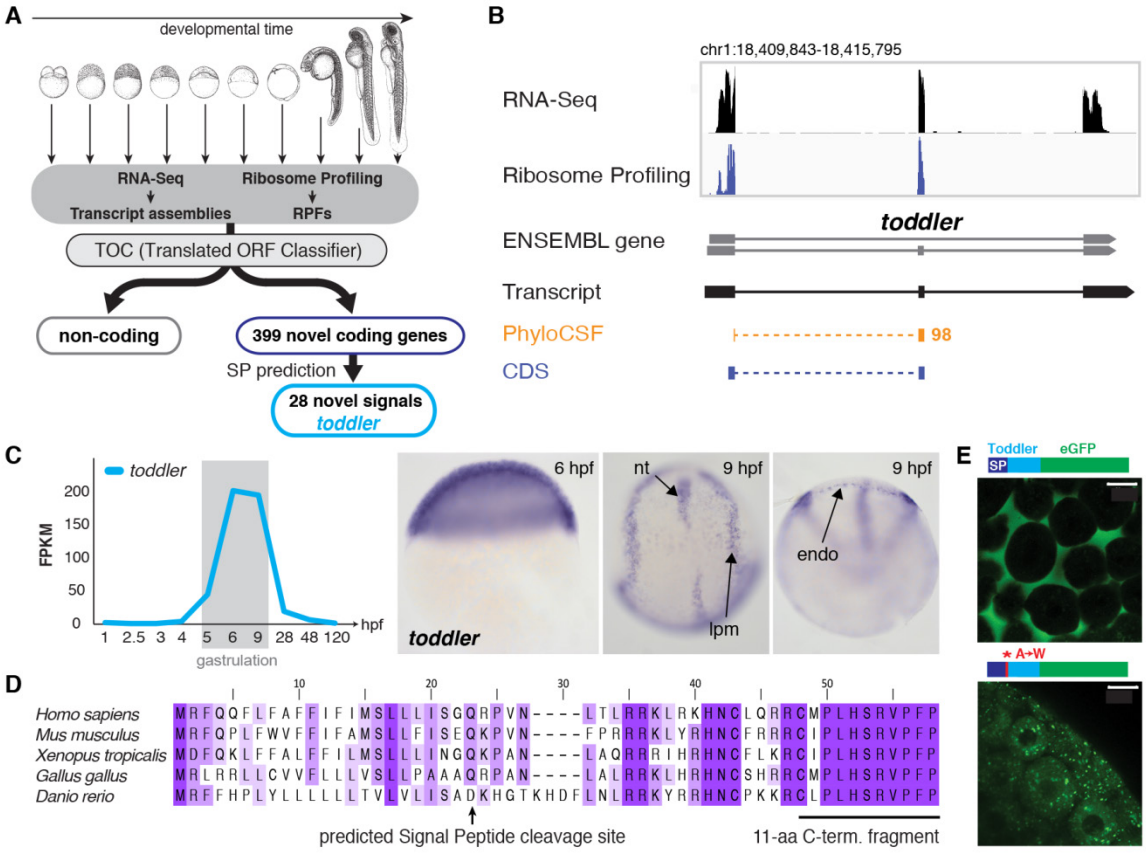

Fig. 1. Identification of the novel embryonic signal Toddler. (**A**) Overview of the individual steps used to identify novel coding and non-coding transcripts. SP, signal peptide; RPFs, ribosome protected fragments. (**B**) Genomic features of *toddler*. Coverage tracks for RNA-Seq (black) and ribosome profiling (blue), and tracks outlining the highest scoring regions in PhyloCSF (orange). Note that both PhyloCSF and ribosome profiling predict *toddler* to be protein-coding. (**C**) Expression analysis of *toddler* transcripts during embryogenesis. *toddler* transcripts peak during gastrulation (RNA-Seq data (*8*); FPKM = Fragments Per Kilobase of transcript per Million mapped reads). RNA in situ hybridization reveals ubiquitous expression of *toddler* transcripts at the beginning of gastrulation (6 hours post fertilization (hpf)); expression becomes restricted to mesendodermal cells toward the end of gastrulation (9 hpf). nt: notochord; lpm: lateral plate mesoderm; endo: endoderm. (**D**) Toddler is conserved in vertebrates. ClustalW2 multiple protein sequence alignment of Toddler peptide sequences from five vertebrates. Darker shading indicates higher percentage identity of the amino acid. The predicted signal peptide cleavage site and the highly conserved C-terminal 11-amino acid (aa) peptide fragment that was detected by mass spectrometry are indicated. (**E**) Toddler signal sequence drives secretion. Injection of mRNAs encoding C-terminal Toddler-eGFP fusion proteins reveal that the wild-type Toddler signal sequence drives secretion (extracellular localization of eGFP), whereas mutation of A->W in the signal peptide (SP) cleavage site causes Toddler-eGFP to remain intracellularly (top: wild-type Toddler ORF; bottom: A->W mutant Toddler ORF). Fusion protein diagrams are not drawn to scale. Scale bars, 20 μm.

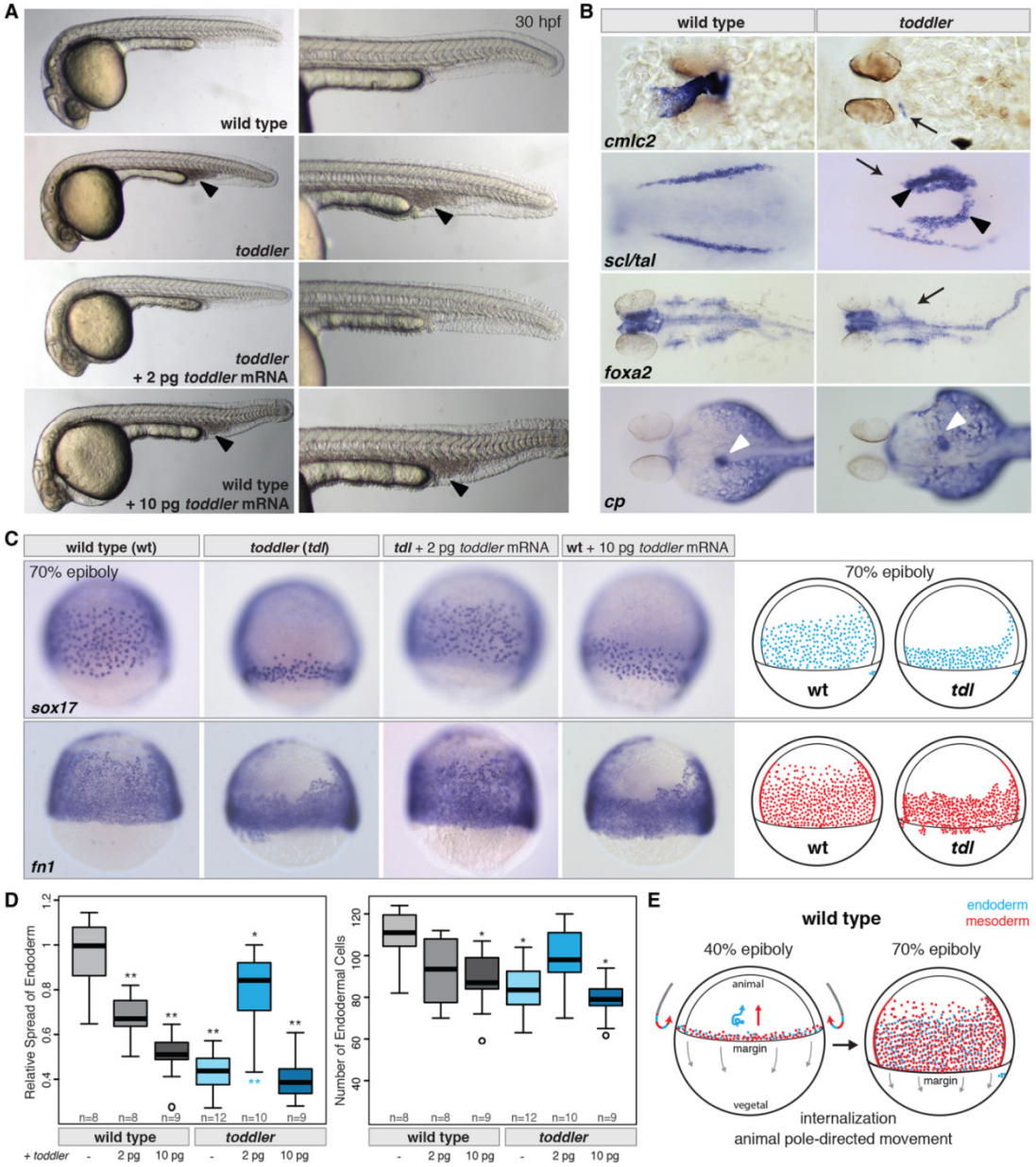

Fig. 2. Toddler is essential for embryogenesis. (**A**) Morphological analysis of *toddler* mutants. TALEN-induced *toddler* null mutants (see fig. S5) lack a functional heart, have no blood circulation and accumulate blood posteriorly (black arrowheads). Defects in *toddler* mutant embryos are rescued by low doses (2 pg) of *toddler* mRNA. Injection of higher doses of *toddler* mRNA (≥ 10 pg) causes phenotypes in wild-type embryos reminiscent of *toddler* loss-of-function mutants. Shown are lateral views of embryos of the indicated genotypes at 30 hours post fertilization. (**B**) Marker gene analysis in wild-type and *toddler* mutant embryos at 36 hpf (*cmlc2*), at the 8-10 somite stage (*scl/tal*), at 30 hpf (*foxa2*) and at 3 days post fertilization (*ceruloplasmin (cp)*). Black arrows indicate lack of or reduced staining in *toddler* mutant embryos; black arrowheads indicate ectopic expression; white arrowheads point to the liver in wild-type (>70% on left side) and *toddler* mutant embryos (expression: 45% right, 15% medial, 40% none/non-specific). (**C**) Toddler is required for movement of ventrolateral endoderm and mesoderm toward the animal pole. Both absence of Toddler (*toddler*) and overexpression of *toddler* mRNA (wild-type embryos + 10 pg *toddler* mRNA) reduces the movement of endodermal (*sox17*) and mesodermal (*fibronectin 1* (*fn1*)) cells toward the animal pole, as detected by in situ hybridization. All in situ images are lateral views of embryos at 70% epiboly (dorsal to the right). Illustrations of the observed endodermal (blue) and mesodermal (red) phenotypes in wild-type (wt) and *toddler* mutant (*tdl*) embryos are shown on the right. (**D**) Quantification of the endodermal defects at 70% epiboly. Left: relative spread of lateral endoderm along the animal-vegetal axis (i.e., height of lateral band of *sox17* expressing cells divided by the wild-type mean); right: number of endodermal cells within a lateral, fixed-size area. Wild-type genomic background, grey; *toddler* mutant genomic background, cyan. p-values for pairwise comparisons with wild type (black, top) or *toddler* mutant (cyan, bottom) were calculated based on a standard Welch's *t* test (* p-value < 0.01; ** p-value < 0.00001). (**E**) Illustration of early gastrulation movements in wild-type zebrafish embryos. Mesodermal (red) and endodermal (blue) cells are induced and internalize at the margin (40% epiboly stage). Whereas internalized cells migrate toward the animal pole either in a directional (mesoderm) or random walk-like pattern (endoderm) (*3*, *15*), epiboly movements are directed toward the vegetal pole (grey arrows). At 70% epiboly, mesodermal and endodermal cells have moved animally and cover most of the lateral side of the embryo.

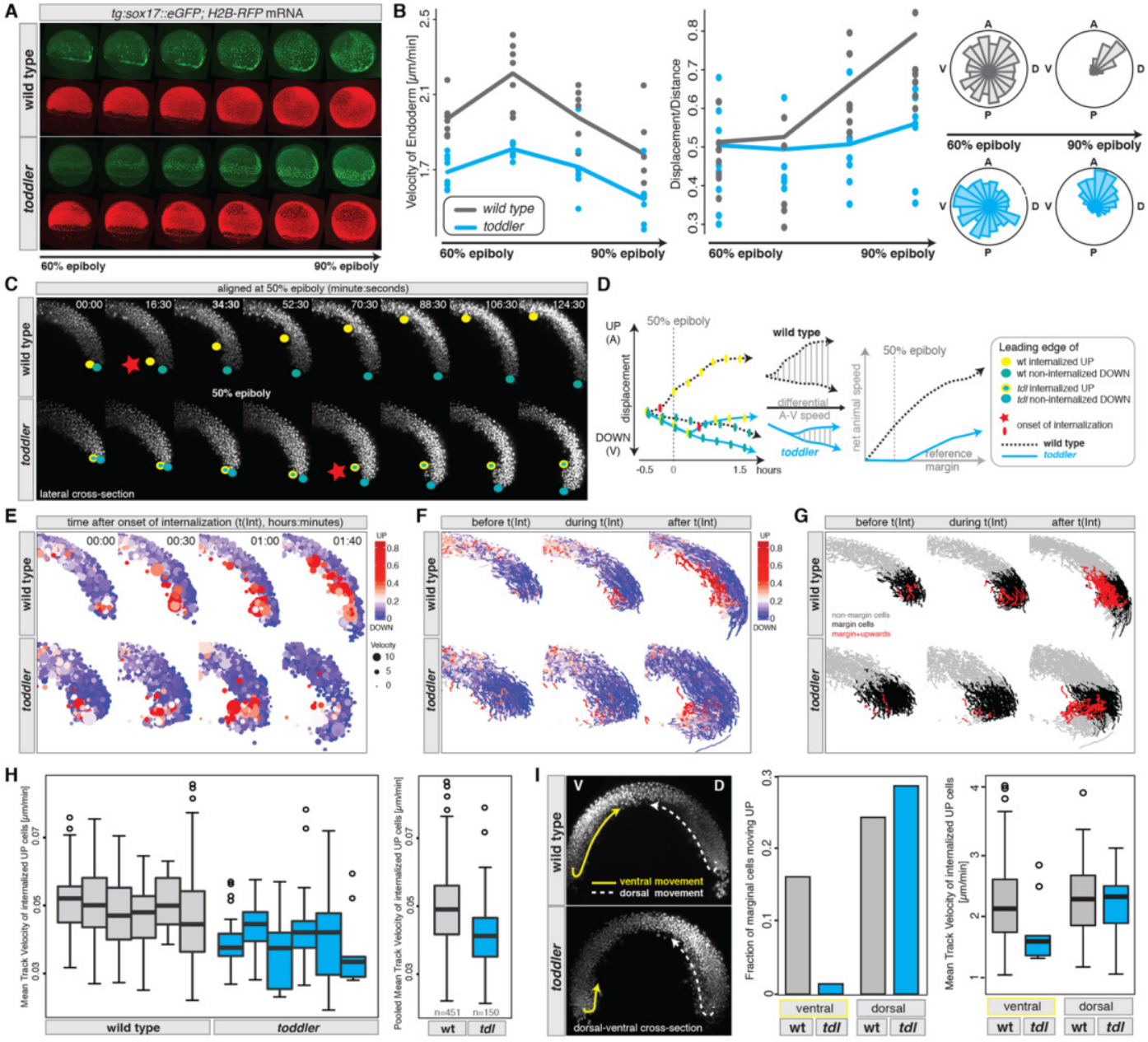
A
tg:sox17::eGFP; H2B-RFP mRNA
wild type
toddler
60% epiboly
90% epiboly
B
Velocity of Endoderm [µm/min]
wild type
toddler
Displacement/Distance
60% epiboly
90% epiboly
A
V
D
P
C
aligned at 50% epiboly (minute:seconds)
00:00
16:30
34:30
52:30
70:30
88:30
106:30
124:30
50% epiboly
lateral cross-section
D
UP (A)
DOWN (V)
displacement
-0.5
0
1.5
hours
differential A-V speed
net animal speed
reference margin
Leading edge of
wt internalized UP
wt non-internalized DOWN
tdl internalized UP
tdl non-internalized DOWN
onset of internalization
E
time after onset of internalization (t(Int), hours:minutes)
00:00
00:30
01:00
01:40
UP
DOWN
Velocity
F
before t(Int)
during t(Int)
after t(Int)
G
non-margin cells
margin cells
margin+upwards
H
Mean Track Velocity of internalized UP cells [µm/min]
wild type
toddler
Pooled Mean Track Velocity of internalized UP cells [µm/min]
n=451
n=150
wt
tdl
I
ventral movement
dorsal movement
dorsal-ventral cross-section
Fraction of marginal cells moving UP
ventral
dorsal
Mean Track Velocity of internalized UP cells [µm/min]

Fig. 3. Abnormal gastrulation movements in *toddler* mutants. (**A** and **B**) Analysis of endodermal cell migration in *sox17::eGFP* transgenic wild-type and *toddler* mutant embryos by confocal microscopy. Endodermal cells (marked by *sox17::eGFP*), green; nuclei (*human Histone2B-RFP* (*H2B-RFP*) mRNA injection), red. (**A**) Still images of maximum intensity projections of a timelapse movie from 60% to 90% epiboly (movies S1 and S2). (**B**) Quantification of the average (median) velocity of endodermal cells (left), displacement versus distance travelled (middle) and directionality (roseplots; right) in wild-type (grey) and *toddler* mutant (cyan) embryos. Each dot represents the average speed (or the ratio between displacement versus distance travelled) of all endodermal cells tracked within a single embryo during a 45-min time interval with respect to its previous position (speed = actual distance (microns)/time (min)). Shown is the data for four consecutive 45-min time windows. Roseplots display the random movement of endodermal cells during early gastrulation and the more directional migration at later stages (animal (A), posterior (P), dorsal (D), ventral (V)). (**C** to **I**) Analysis of early gastrulation movements in *H2B-RFP* mRNA injected wild-type and *toddler* mutant embryos by light-sheet microscopy (Single Plane Illumination Microscopy (SPIM)). In (C) to (H), internalization and animal pole-directed movement of lateral mesendodermal cells is reduced in *toddler* mutants. Analyses are shown for lateral cross-sections of a timelapse movie (movie S4) of a wild-type – *toddler* mutant embryo pair, imaged in parallel at 90 s intervals within a single experiment. (**C**) Still images of maximum intensity projections of 40 µm lateral cross-sections (20 z-slices) during the time of internalization (time in minutes:seconds). Movies were aligned at 50% epiboly (48:00). Leading edges of internalizing mesendodermal cells (yellow dots) and vegetally moving cells (green dots) highlight the opposing paths of cells during gastrulation. Red stars mark the onset of cell internalization. (**D**) Comparison of animally and vegetally directed migratory paths of the wild-type and mutant embryo pair shown in (C). Frame-to-frame displacements (plotted on the left) were used to derive the net animal pole-directed cell movement. *Toddler* mutants (cyan) show delayed onset of internalization and reduced step-to-step and net animal pole-directed movement. (**E** to **G**) Cell tracking and digital analysis of gastrulation movements. (**E**) Position, speed (dot size) and directionality (color-code from blue (vegetal movement) to red (animal movement)) of tracked cells during and after the time of internalization (t(Int)). Movies were aligned to the onset of internalization (t(Int) = 00:00; time in hours:minutes). (**F** and **G**) Cell tracks before (t < -5 min), during (-5 min < t < 1h), and after (t > 1h) internalization in wild-type and *toddler* mutant embryos. In (**F**), tracks were color-coded based on the total number of animal pole- (red) or vegetal pole- (blue) directed movements, normalized to the total number of frames per track. In (**G**), tracks were color-coded based on their relative position and directionality with respect to the margin at the time of internalization (margin cells: cells located within 100 µm above the margin at the onset of internalization). Non-margin cells, grey; margin cells, black; internalizing and upwards-moving margin cells, red. (**H**) Quantification of the mean velocity of internalizing, animal pole-directed movement in wild-type and toddler mutant embryos. Mean track velocities were obtained from cell tracking data derived from lateral cross-sections of 6 wild-type (grey) and 6 *toddler* mutant (cyan) embryos, imaged in parallel in three independent experiments. Pooled wild-type and *toddler* mutant mean track velocities are plotted on the right (n = number of cell tracks). (**I**) *Toddler* mutant embryos are defective in ventrolateral but not dorsal internalization. (Left) Still image of maximum intensity projections of 40 µm dorsal-ventral cross-sections (20 z-slices) of a wild-type - *toddler* mutant embryo pair 110 min after the onset of internalization. Arrows highlight the paths that the leading internalizing cells took on dorsal (D, dashed white line) and ventral (V, solid yellow line) sides of the embryo. Ventral movement toward the animal pole is severely reduced in the *toddler* mutant embryo, while dorsal internalization occurs normally. (Right) Quantification of the fraction and speed of internalizing marginal cells based on their positioning in the embryo (dorsal versus ventral) and genotype (wild type (grey) versus *toddler* mutant (cyan)) (see also movie S6).

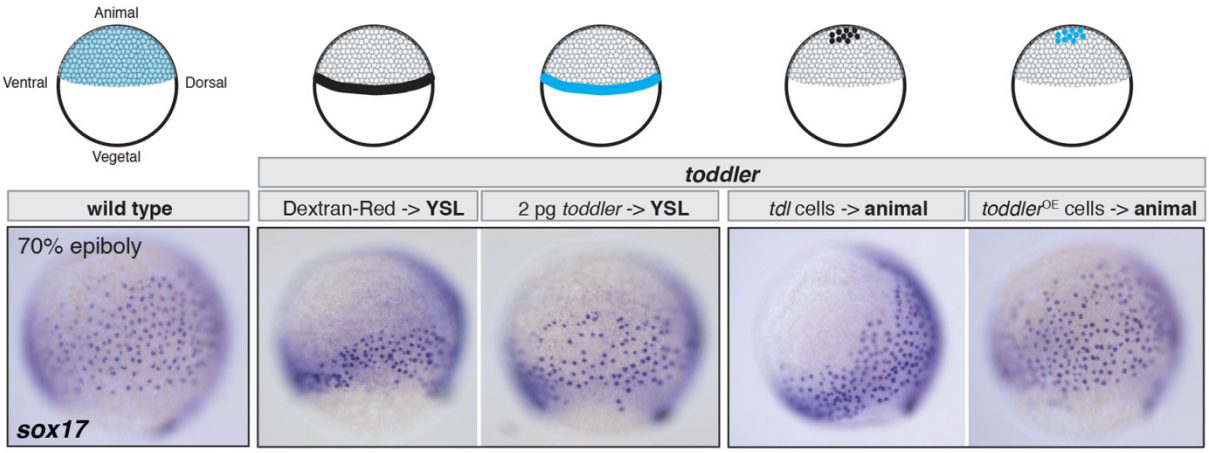

Fig. 4. Toddler functions as a motogen. Ubiquitous or localized expression of Toddler promotes animal pole-directed endodermal cell migration in *toddler* mutant embryos. Toddler was either expressed vegetally from the yolk syncytial layer (YSL) (injection of *toddler* mRNA into the YSL) or animally from a *toddler*-overexpressing (OE) clone of cells transplanted into the animal pole. Dextran-Red injections into the YSL and transplantation of uninjected *toddler* mutant cells served as controls. Different treatments are illustrated on top; *toddler* expression domains are highlighted in cyan. All *sox17 in situ* hybridization images are lateral views of embryos at 70% epiboly (dorsal to the right).

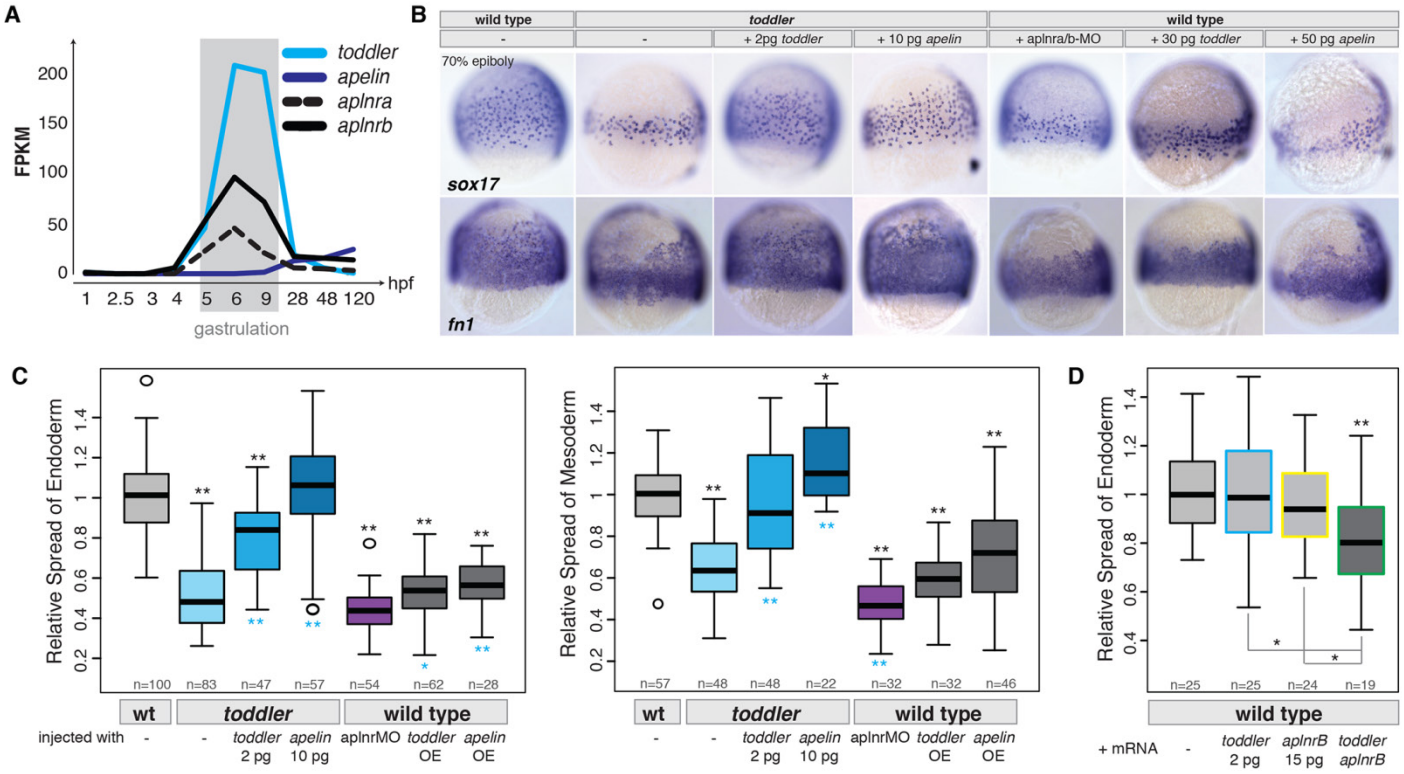

Fig. 5. Toddler acts via Apelin receptors. (**A**) RNA-Seq-based expression levels of *toddler, apelin,* and *apelin receptors (aplnra* and *aplnrb*) during embryogenesis. FPKM = Fragments Per Kilobase of transcript per Million mapped reads. (**B**) Genetic evidence for Toddler signaling via the Apelin receptor. Endodermal (*sox17*) and mesodermal (*fibronectin 1* (*fn1*)) cell distributions were analyzed by in situ hybridization at 70% epiboly. Apelin receptor knockdown (aplnra/b morpholino (MO) injection) phenocopies *toddler* mutants, and Apelin production can rescue *toddler* mutants. Overexpression of Apelin causes phenotypes resembling *toddler* mRNA overexpression. (**C**) Quantification of the relative lateral spread of endoderm (left) and mesoderm (right). Quantifications are from multiple experiments (n = number of embryos per category). p-values for pairwise comparisons with wild type (black, top) or *toddler* mutant (cyan, bottom) were calculated based on a standard Welch's *t* test (* p-value < 0.01; ** p-value < 0.00001). (**D**) Synergistic effect of Toddler and Apelin receptor b on endodermal cell migration. Injection of *toddler* or *aplnrb* mRNA at low concentrations (2 pg and 15 pg, respectively) did not cause significant defects in animal pole-directed movement of endodermal cells (different batch of *toddler* mRNA than used in Fig. 2D). However, co-injection of both mRNAs reduced the extent of endoderm movement. Shown is the combined data of two independent experiments. p-values for pairwise comparisons with wild type (top) or individual mRNA injections (bottom) were calculated based on a standard Welch's *t* test (* p-value < 0.01; ** p-value < 0.00001).

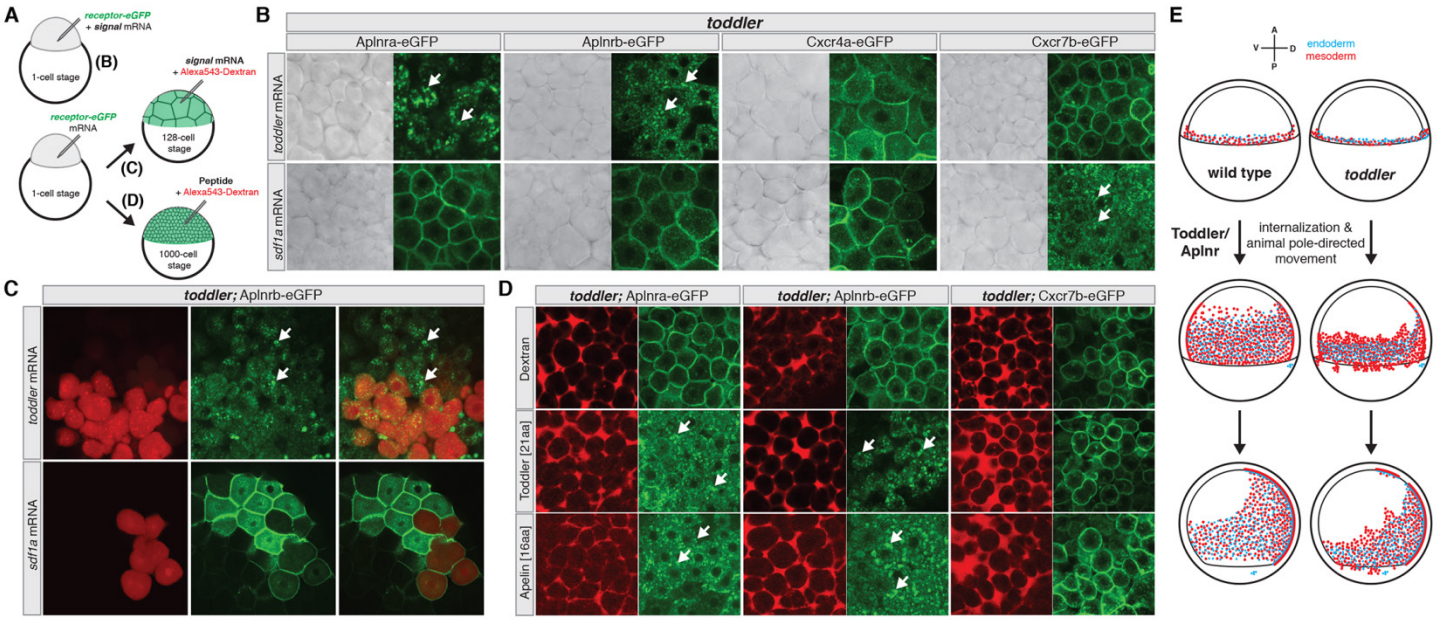

Fig. 6. Toddler drives internalization of Apelin receptors. (**A**) Schematic illustration of different treatments used to test for Toddler-mediated Apelin receptor internalization. (**B**) Test for signal-mediated internalization of eGFP-tagged receptors in zebrafish by coinjection of *signal* and *receptor-eGFP* mRNA into one-cell stage *toddler* mutant embryos. Receptor internalization was monitored by confocal microscopy. White arrows point to fluorescent foci of internalized receptors. In the absence of signal peptide overexpression, ectopically expressed receptors localize to the plasma membrane in pre-gastrulation *toddler* mutant embryos (see control Alexa543-Dextran injections in Fig. 6D). (**C**) Generation of a local source of Toddler or Sdf1a by injection of *toddler* or *sdf1a* mRNA (together with Alexa543-Dextran as tracer) into a single cell at the 128-cell stage. Local expression of Toddler is sufficient to cause Aplnrb-eGFP internalization in cells that do not express *toddler* mRNA (non-red cells). (**D**) Extracellular injection of in vitro synthesized C-terminal Toddler or Apelin peptide fragments is sufficient to drive internalization of Apelin receptors. (**E**) Model of the role of Toddler-Apelin receptor signaling in mesendodermal cell migration during zebrafish gastrulation. Wild-type, left; *toddler*, right; 40% epiboly (mesendoderm specification and internalization), top; 70% epiboly (animal pole-directed cell movement), middle; 90% epiboly (dorsal convergence), bottom.